

Recoil corrections in antikaon-deuteron scattering

Maxim Mai^a, Vadim Baru^{b,c}, Evgeny Epelbaum^b, Akaki Rusetsky^a

^a*Helmholtz-Institut für Strahlen- und Kernphysik (Theorie) and Bethe Center for Theoretical Physics, Universität Bonn, D-53115 Bonn, Germany*

^b*Institut für theoretische Physik II, Fakultät für Physik und Astronomie, Ruhr-Universität Bochum, 44780 Bochum, Germany*

^c*Institute for Theoretical and Experimental Physics, 117218, B. Cheremushkinskaya 25, Moscow, Russia*

Abstract

The recoil retardation effect in the K^-d scattering length is studied. Using the non-relativistic effective field theory approach, it is demonstrated that a systematic *perturbative* expansion of the recoil corrections in the parameter $\xi = M_K/m_N$ is possible in spite of the fact that K^-d scattering at low energies is inherently non-perturbative due to the large values of the $\bar{K}N$ scattering lengths. The first order correction to the K^-d scattering length due to single insertion of the retardation term in the multiple-scattering series is calculated. The recoil effect turns out to be reasonably small even at the physical value of $M_K/m_N \simeq 0.5$.

Keywords: Antikaon-deuteron scattering; Multiple scattering series; Non-relativistic effective field theories; Nucleon recoil;

PACS: 36.10.Gv, 13.75.Cs, 13.75.Jz

1. Introduction

Antikaon-nucleon scattering is an excellent testing ground for understanding the $SU(3)$ QCD dynamics at low energies in the one-baryon sector. Starting from the seminal paper [1], it is often described within the so-called unitarized Chiral Perturbation Theory (ChPT), which uses the chiral potential calculated at a certain order (see, e.g., Refs. [2–10]). Different versions of the unitarized ChPT are available in literature. However, a common feature of all formulations is a relatively large number of free parameters, which are fixed from the fit to the experimental data. An important part of the input is coming from the S-wave $\bar{K}N$ scattering lengths, which “nail down” the amplitudes at the $\bar{K}N$ threshold and thus impose stringent constraints both on the scattering in the $\bar{K}N$ channel as well as the sub-threshold behavior of the amplitudes. The latter plays an important role in the study of the interaction of the K^- with nuclear medium (see, e.g., Ref. [11]).

The experiments with kaonic atoms have been carried out in order to extract the precise values of the S-wave $\bar{K}N$ scattering lengths – a goal that could be hardly achieved by using different experimental techniques. Recently, the energy shift and width of kaonic hydrogen were measured very accurately in the SIDDHARTA experiment at DAΦNE [12] (for the earlier attempts, see, e.g., Refs. [13, 14]). These two quantities can be related to the K^-p scattering lengths via the so-called modified Deser-type formula, see Refs. [15, 16] (a general discussion of the procedure of extracting the scattering lengths from the hadronic atom observables can be found, e.g., in a review article [17]). The same experimental collaboration has made an attempt to measure the energy and the width of the ground state of the kaonic deuterium as well. However, due to a small signal-to-background ratio, no clear signal from the kaonic deuterium was detected [18]. Only an upper limit on the yield of the kaonic deuterium K_α line could be determined which is important for the evaluation of the new experiments proposed at LNF [19] and J-PARC [20]. In addition, the kaonic ^3He and ^4He atoms have also been studied within the SIDDHARTA experiment.

What makes the experiments with kaonic deuterium extremely important is the fact that the S-wave $\bar{K}N$ scattering lengths are complex-valued, in difference, e.g., to the πN scattering lengths, which are real quantities. The πN scattering lengths can be, in principle, determined directly on the basis of π^-H data alone [21] while the level shift of the pionic deuterium [22] is used as a complementary information to improve the accuracy in the extraction of the πN scattering lengths, see Ref. [23] for the results of the latest combined analysis of pionic atoms. Meanwhile, extracting two complex scattering lengths a_0, a_1 corresponding to the total isospin $I = 0, 1$ in the $\bar{K}N$ system implies

the determination of four real quantities and thus requires measurements of four independent observables. Two observables are provided by the kaonic hydrogen, and the remaining two can come from, e.g., the kaonic deuterium. The problem is, however, that the kaonic deuterium measurement would yield the $\bar{K}d$ scattering length, and there is still a long way to go from this quantity to the $\bar{K}N$ scattering lengths. Thus, unless one is able to relate the $\bar{K}d$ and $\bar{K}N$ scattering lengths with each other with a controlled accuracy using a consistent theoretical framework, the main goal of the kaonic deuterium experiment can not be achieved.

In the past decades, the calculations of the low-energy $\bar{K}d$ scattering observables within the non-relativistic three-body Faddeev framework have reached an unprecedented accuracy and sophistication (see here an incomplete list of papers on this subject: [24–30]). However, despite all efforts, these calculations do not address the core issue, which consists in the feasibility of the extraction of the $\bar{K}N$ scattering lengths from data. To this end, one needs an explicit expression of the $\bar{K}d$ scattering length in terms of the $\bar{K}N$ scattering lengths of the type of Brueckner formula [31], see also Ref. [32]. Based on this expression, in Refs. [33, 34] the extraction of the $\bar{K}N$ scattering lengths from the combined data on the kaonic hydrogen and kaonic deuterium has been analyzed. It should be however stressed that the expression derived in Refs. [31–33] is only an approximation and assumes that nucleons are infinitely heavy (static). There exists no *a priori* reason to believe that this is a good approximation, especially in view of the fact that, in the real world, the mass ratio $M_K/m_N \simeq 0.5$ is not small. On the other hand, *numerical* estimates, carried out within the Faddeev approach, indicate that this approximation might be not so bad as it seems at the first glance (see Ref. [35]). One therefore may conclude that, in order to have a *reliable* estimate of the uncertainty of the method, it is necessary to have a systematic framework for calculating corrections to the static limit. This issue has been first addressed in Ref. [36], where the recoil corrections in the double scattering process have been studied within the non-relativistic field-theoretical approach. This paper represents a continuation and extension of the work started in Ref. [36].

Below we list some fundamental questions that the systematic theory of kaonic deuterium should be able to answer in the future:

- i) $\bar{K}d$ scattering at low energies is inherently non-perturbative due to the large values of the S-wave $\bar{K}N$ scattering lengths, so a re-summation of the multiple scattering series is necessary (in difference, e.g., to πd scattering, where a perturbative approach is justified). Such re-summation, however, can be carried out analytically only in the static limit. Bearing in mind that $M_K/m_N \simeq 0.5$, it is legitimate to ask, how should the recoil corrections be systematically taken into account in the above non-perturbative scheme.
- ii) Numerical estimates in the potential models show that the size of the recoil correction is moderate, despite the fact that the kaon is quite heavy. One has to understand this observation on the basis of robust theoretical arguments.
- iii) The effective low-energy theory of QCD is ChPT. Since experiments probe predictions of QCD, the theoretical framework used to analyze the data, should be chosen accordingly. This means, e.g., that the nucleon-nucleon and kaon-nucleon interactions should be described on the basis of effective chiral Lagrangians. Because of non-perturbative character of NN and $\bar{K}N$ interactions, it could be however prohibitively complicated to try to describe the three-body dynamics of the $\bar{K}d$ system directly in ChPT. In Ref. [36] we have formulated an alternative approach, based on the use of the non-relativistic (non-local) effective Lagrangian, which have the (chiral) two- and three-body potentials as an input, see Sec.2 for more details. Calculations of the $\bar{K}d$ scattering length can be systematically done within this approach.
- iv) The presence of the sub-threshold $\Lambda(1405)$ resonance in $\bar{K}N$ scattering does not only lead to large scattering length. It also causes a rapid variation of the amplitudes near threshold. Therefore a systematic study of the (potentially large) effective-range corrections is required.
- v) In the effective field theory approach, the three-body forces are necessarily present and guarantee independence of physical observables on the renormalization scale. Consequently, a reliable estimate of this contribution to the $\bar{K}d$ scattering length is needed, see Refs.[36, 37] for further discussions of this subject.

In the present paper, we concentrate on the study of the recoil effect and leave other issues for future publications. In particular, our main aim is to formulate a procedure for including the recoil corrections *perturbatively* into the multiple-scattering series, in which the static interactions are summed up *to all orders*.

The paper is organized as follows. In section 2 we discuss the general scheme of including the recoil corrections into the multiple-scattering series and discuss the counting scheme for such corrections. In section 3, we derive the formulae for the single insertion of the recoil correction in the multiple-scattering series. Explicit derivation of the formulae for $\bar{K}d$ scattering is given in section 3, where the numerical results for one “recoil insertion” are also shown. In section 4, we discuss the expansion of a single recoil insertion in the (non-integer) powers of the parameter $\xi = M_K/m_N$, along the similar lines to Ref. [36], and demonstrate the convergence of this expansion. In section 5, the numerical results for the first-order recoil correction to the $\bar{K}d$ scattering length are presented. Furthermore, we also calculate the boundaries for the antikaon-deuteron scattering length using various $\bar{K}N$ scattering lengths existing in the literature as an input. The section 6 contains our conclusions.

2. Theoretical framework

The starting point of the analysis is the generalized Deser-type relations between the energy shift/width of the $1s$ level of the kaonic hydrogen ($\Delta E_{1s}, \Gamma_{1s}$) and kaonic deuterium ($\Delta E_{1s}^d, \Gamma_{1s}^d$) and the pertinent $\bar{K}N$ and $\bar{K}d$ threshold amplitudes. These relations are well known in the literature (see, e.g., Refs. [15–17, 33]) and, at order $O(\alpha)$ in isospin breaking, take the form

$$\begin{aligned}\Delta E_{1s} - i\Gamma_{1s}/2 &= -2\alpha^3\mu^2 a_p(1 - 2\mu\alpha(\ln\alpha - 1)a_p), \\ \Delta E_{1s}^d - i\Gamma_{1s}^d/2 &= -2\alpha^3\mu_d^2 \mathcal{A}(1 - 2\mu_d\alpha(\ln\alpha - 1)\mathcal{A}),\end{aligned}\tag{1}$$

where μ and μ_d are the reduced masses, and a_p and \mathcal{A} are the threshold amplitudes of the $\bar{K}N$ and $\bar{K}d$ systems, respectively. Moreover, it can be shown (see Ref. [36]) that all logarithmically enhanced terms of type $\alpha^n \ln^n \alpha$ for $n = 1, 2, \dots$ can be re-summed to all orders, which leads to the replacement $1 - 2\mu\alpha(\ln\alpha - 1)a_p \rightarrow (1 + 2\mu\alpha(\ln\alpha - 1)a_p)^{-1}$ and, similarly, to the replacement $1 - 2\mu_d\alpha(\ln\alpha - 1)\mathcal{A} \rightarrow (1 + 2\mu_d\alpha(\ln\alpha - 1)\mathcal{A})^{-1}$. This procedure substantially improves the agreement between the modified Deser formulae and the explicit solutions within the framework of the potential models both for the kaonic hydrogen and kaonic deuterium¹.

As seen from the above formulae, the measurement of the energy shift and width of the kaonic hydrogen allows one to directly determine the (complex) K^-p scattering length a_p that fixes two of four relations on the S-wave $\bar{K}N$ scattering lengths a_0 and a_1 . The remaining two relations must be provided from the eventually measured value of \mathcal{A} . A systematic expansion of the antikaon-deuteron scattering length in terms of the $\bar{K}N$ scattering lengths (and higher-order effective-range expansion parameters) naturally emerges through the perturbative expansion of the threshold amplitude \mathcal{A} in the non-relativistic effective field theories. The resulting scattering length is written in a form of a sum of all six-point $\bar{K}NN \rightarrow \bar{K}NN$ diagrams, folded by the deuteron wave functions, and effective couplings in these diagrams in a particular renormalization scheme can be expressed in terms of the $\bar{K}N$ scattering lengths, effective radii and so on. However, due to the large values of the $\bar{K}N$ scattering lengths, the resulting multiple-scattering series for the six-point function does not converge. The only case when the multiple-scattering series can be algebraically re-summed to all orders, is the so-called static approximation $m_N \rightarrow \infty$. In this limit, the answer is explicitly written as [32, 33]²

$$\mathcal{A}_{\text{st}} = \frac{1}{1 + \xi/2} \int d^3\mathbf{r} |\Psi(\mathbf{r})|^2 \frac{\tilde{a}_n + \tilde{a}_p + (2\tilde{a}_p\tilde{a}_n - b_x^2)/r - 2b_x^2\tilde{a}_n/r^2}{1 - \tilde{a}_p\tilde{a}_n/r^2 + b_x^2\tilde{a}_n/r^3}.\tag{2}$$

Here, $\Psi(r)$ stands for the wave function of the deuteron, normalized to unity. In momentum space, it obeys the equation

$$(\gamma^2 + \mathbf{p}^2)\Psi(\mathbf{p}) = \frac{1}{4m_N} \int \frac{d^3\mathbf{q}}{(2\pi)^3} V_{NN}(\mathbf{p}, \mathbf{q})\Psi(\mathbf{q}),\tag{3}$$

¹We thank A. Cieplý for the advanced communication of his numerical results to us.

²In the kinematical prefactor, which appears in the r.h.s. of Eq. (2), we have neglected the deuteron binding energy as compared to the nucleon mass.

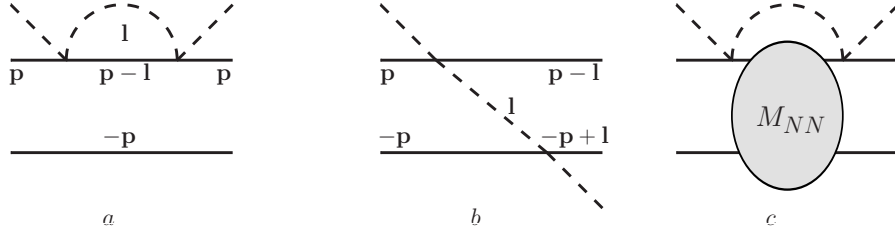


Figure 1: The types of the diagrams emerging in the multiple-scattering series: a) the self-energy type diagram; b) the exchange diagram; c) any number of the “potential exchanges” between two nucleons in the intermediate state.

where $\gamma^2 = m_N \varepsilon_d$ is the bound-state momentum in the deuteron while ε_d denotes the binding energy. Further,

$$\tilde{a}_{p,n,x,u} = (1 + \xi) a_{p,n,x,u}, \quad b_x^2 = \tilde{a}_x^2 / (1 + \tilde{a}_u / r), \quad (4)$$

where $a_{p,n,x,u}$ are the $\bar{K}N$ scattering lengths in the different physical channels $K^- p \rightarrow K^- p$, $K^- n \rightarrow K^- n$, $K^- p \rightarrow \bar{K}^0 n$ and $\bar{K}^0 n \rightarrow \bar{K}^0 n$, respectively. In the isospin symmetry limit, $a_p = a_u = (a_0 + a_1)/2$, $a_n = a_1$, $a_x = (a_1 - a_0)/2$. Numerically, in most cases, Eq. (2) is a rather good approximation to the exact solution in spite of the relatively large kaon mass. In this paper, we demonstrate that the recoil corrections can be calculated perturbatively, order by order even though the original multiple-scattering series (MSS) is inherently non-perturbative. Below, we describe, how this goal can be achieved.

An appropriate framework to this problem is the one based on the non-relativistic effective Lagrangians. We have described this framework in detail in Ref. [36]. Here we only briefly mention the crucial properties of the approach, focusing on the aspects which are new.

The approach relies on the existence of two distinct momentum scales. The nucleon-nucleon and three-particle interactions are characterized by a low scale (of the order of the pion mass) and are described by non-local, energy-independent potentials $V_{NN}(\mathbf{p}, \mathbf{q})$ and $V_3(\mathbf{p}_1, \mathbf{p}_2, \mathbf{p}_3; \mathbf{q}_1, \mathbf{q}_2, \mathbf{q}_3)$, respectively. It is understood that, ultimately, these potentials should be taken from chiral effective field theory in the two-nucleon sector. In the actual calculations carried out in this paper we shall, however, use phenomenological nucleon-nucleon forces which yield results similar to the chiral potentials and are easier to handle. On the contrary, $\bar{K}N$ interactions are characterized by a heavier scale (of the order of the mass of the ρ, ω, \dots resonances). We shall describe these interaction by a tower of local terms in the Lagrangian with zero, two, \dots space derivatives. The couplings emerging in these terms are expressed through the $\bar{K}N$ scattering lengths, effective radii and so on in a standard manner. For this reason, a *perturbative* expansion in such an effective theory automatically yields the *multiple-scattering series*, known from the potential scattering framework. The leading contribution to this series is provided by the term with no derivatives which after re-summation yields Eq. (2).

A generic term in the multiple-scattering expansion contains the diagrams in which the kaons are exchanged between two nucleons as well as kaons hopping on the same nucleon (the self-energy-type diagrams), see Fig. 1. Since NN interactions are non-perturbative, they have to be included to all orders. This is normally done by solving the Lippmann-Schwinger type equations which yield the NN amplitudes at low-energies. The NN amplitude in its turn is to be included in each intermediate state of the $\bar{K}NN - \bar{K}NN$ Feynman diagrams, see e.g. diagram c in Fig.1.

The renormalization prescription in the $\bar{K}N$ sector should guarantee that the self-energy loop shown in Fig. 1a vanishes at threshold in the $\bar{K}N$ center of mass frame. Indeed, the self-energy loop in the two-body sector is already included as a part of the relation between the effective coupling in the Lagrangian and the scattering length. Therefore in the calculation of the $\bar{K}NN - \bar{K}NN$ Feynman diagrams where the $\bar{K}N$ scattering lengths are used in the vertices only that part of the loop survives which appears due to the presence of the 3-body dynamics. The procedure was described in detail, e.g., in Ref. [38] using πN scattering as an example. Using time-ordered perturbation theory, the expression for the self-energy diagram is given in the form

$$J_{S.E.}(\mathbf{p}^2, E) = \int_{\text{reg}} \frac{d^3 \mathbf{l}}{(2\pi)^3} \frac{1}{\mathbf{l}^2 / 2M_K + (\mathbf{p} - \mathbf{l})^2 / 2m_N + \mathbf{p}^2 / 2m_N - E - i0}$$

$$= \int_{\text{reg}} \frac{d^3\mathbf{l}}{(2\pi)^3} \frac{1}{\mathbf{l}^2/2\mu + \mathbf{p}^2/2(m_N + M_K) + \mathbf{p}^2/2m_N - E - i0}, \quad (5)$$

where the subscript “reg” stands for some (unspecified) ultraviolet regularization prescription, and E stands for the energy with respect to the $\bar{K}d$ threshold. In order to obtain the second expression, a shift of the integration variable $\mathbf{l} \rightarrow \mathbf{l} + \xi/(1 + \xi)\mathbf{p}$ was necessary. Consequently, the renormalized self-energy (after subtraction of the two-body term) takes the form

$$J_{S.E.}^r(\mathbf{p}^2, E) = \int \frac{d^3\mathbf{l}}{(2\pi)^3} \left\{ \frac{1}{\mathbf{l}^2/2\mu + \mathbf{p}^2/2(m_N + M_K) + \mathbf{p}^2/2m_N - E - i0} - \frac{1}{\mathbf{l}^2/2\mu} \right\}. \quad (6)$$

This expression indeed vanishes in the two-particle center of mass frame at threshold ($\mathbf{p} = 0, E = 0$). On the other hand, when this loop is embedded in the nuclear (deuteron) environment, the energy becomes $E = -\varepsilon_d$, and the nucleon momentum \mathbf{p} does not vanish anymore.

An appropriate parameter to establish the counting scheme for the recoil corrections is $\xi = M_K/m_N$. It can be easily seen that, in the vicinity of the static limit ($\xi \rightarrow 0$) the renormalized self-energy graph vanishes as $O(\xi^{1/2})$. Further, it can be also checked that the operator with NN interactions in the intermediate state, see Fig. 1c, also leads to the contributions suppressed as $O(\xi^{1/2})$. Consequently, in the static limit, only diagrams of the type shown in Fig. 1b survive. These are the diagrams where the kaon is exchanged between two nucleons. In this limit and assuming, in addition, $\varepsilon_d \rightarrow 0$, the three-particle $\bar{K}NN$ propagator in the exchange diagram simplifies to

$$g \doteq \frac{1}{\mathbf{l}^2/2M_K + (\mathbf{p} - \mathbf{l})^2/2m_N + \mathbf{p}^2/2m_N + \varepsilon_d} \rightarrow \frac{1}{\mathbf{l}^2/2M_K}, \quad (7)$$

so that the resulting series can be summed up to all orders. Taking the Fourier transform and folding the result with the deuteron wave function, we finally arrive at the expression displayed in Eq. (2).

Away from the static limit, the propagator in the exchange diagram can be rewritten in the following form

$$g = \frac{1}{\mathbf{l}^2/2M_K} + \left\{ \frac{1}{\mathbf{l}^2/2M_K + (\mathbf{p} - \mathbf{l})^2/2m_N + \mathbf{p}^2/2m_N + \varepsilon_d} - \frac{1}{\mathbf{l}^2/2M_K} \right\} \doteq g_{\text{st}} + \Delta g, \quad (8)$$

where the expression in the curly bracket, which is defined as Δg , stands for the recoil correction. The splitting shown above allows for the perturbative treatment of the recoil effect in the $\bar{K}d$ scattering length. Schematically, the procedure can be described as follows. Consider, for example, the diagrams of a type shown in Fig. 1b. Let \tilde{a} denote a generic $\bar{K}N$ scattering length which is related to the non-derivative coupling in the effective Lagrangian. Then, Feynman diagrams of type b correspond to consecutive scattering of the kaon off different nucleons mediated by the $\bar{K}NN$ Green functions g from Eq. (8), i.e. $\tilde{a}g\tilde{a}\dots$. The multiple-scattering series can be therefore written as

$$\tilde{a} + \tilde{a}g\tilde{a} + \tilde{a}g\tilde{a}g\tilde{a} + \dots = \left\{ \tilde{a} + \tilde{a}^2 g_{\text{st}} + \dots \right\} + \left\{ \tilde{a} + \tilde{a}^2 g_{\text{st}} + \dots \right\} (\Delta g) \left\{ \tilde{a} + \tilde{a}^2 g_{\text{st}} + \dots \right\} + \dots. \quad (9)$$

It is seen that the whole multiple-scattering series can be rearranged so that the static contributions are re-summed to all orders (the expression in the first curly bracket in the r.h.s of Eq. (9)), whereas the recoil corrections enter perturbatively, in the form of one, two, ... “recoil insertions”, see the terms $\sim (\Delta g)^n$, with $n = 1, 2, \dots$. In Sec. 4 we shall prove that each insertion counts as $O(\xi^{1/2})$ (or, in some cases, as $O(\xi)$) and, consequently, to carry out calculations at a given order in the expansion parameter ξ , it suffices to consider a finite number of insertions.

In the above equation, for illustration, only the contribution from the exchange diagram was shown. The contributions from the diagrams shown in Fig. 1a and 1c are parts of the recoil insertions, because they are absent in the static case. We shall see later that they are also vanishing at $O(\xi^{1/2})$.

Diagrams with one recoil insertion, which contribute to the $\bar{K}d$ scattering length are shown explicitly in Fig. 2. The case with two and more insertions can be treated similarly and is beyond the scope of this work.

Up to now, to the best of our knowledge, the recoil insertion has been treated in the literature only within a perturbative EFT framework (see, e.g., [36, 38]). In the present paper, we present the perturbative evaluation of the recoil insertions while the static diagrams are summed up to all orders. Thus, the convergence of the multiple-scattering series is not assumed, and does not hold, in general.

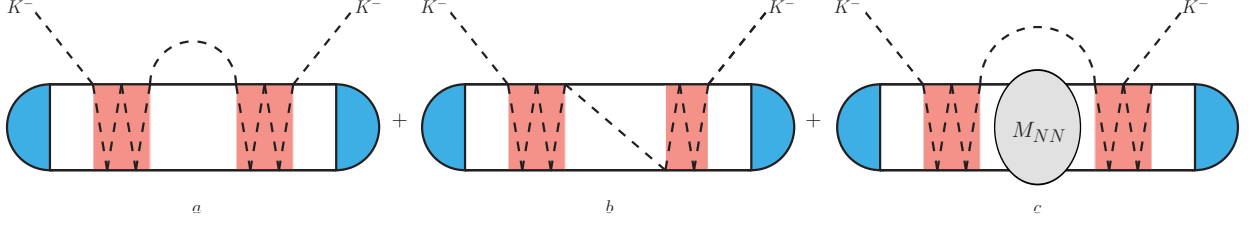


Figure 2: Diagrams with one recoil insertion, where dashed (solid) lines denote the kaon (nucleon) lines, respectively. The whole diagram is folded by the deuteron wave functions (semicircles). The shaded boxes with kaon propagators symbolically denote the re-summed infinite series of kaon exchange graphs in the static limit, whereas the dashed lines outside of the boxes denote the retarded kaon propagators. The nucleon-nucleon amplitude is referred to as M_{NN} .

3. One recoil insertion

In this section, we shall present compact explicit expressions for the recoil insertions in the multiple scattering series. As discussed in the previous section, the antikaon-deuteron scattering length can be written as

$$\mathcal{A} = \mathcal{A}_{\text{st}} + \mathcal{A}^{(1)} + \mathcal{A}^{(2)} + \dots, \quad (10)$$

where the individual terms correspond to the zero, one, two, \dots recoil insertions. The lowest order amplitude corresponding to the static limit was defined by Eq. (2). Next, consider one recoil insertion, as illustrated by the diagrams in Fig. 2. At this order, one has the diagrams a and b , where the kaon scatters either on the same nucleon or on different nucleons, as well as the diagram c which takes into account the intermediate NN interactions to all orders. Consequently,

$$\mathcal{A}^{(1)} = \mathcal{A}^{(a)} + \mathcal{A}^{(b)} + \mathcal{A}^{(c)}, \quad (11)$$

where

$$\begin{aligned} \mathcal{A}^{(a)} &= \frac{1}{1 + \xi/2} \int \frac{d^3 \mathbf{p} d^3 \mathbf{l}}{(2\pi)^6} G_{\text{r}}(\mathbf{p}, \mathbf{l}) \left[\Phi_p^2(\mathbf{p} + \mathbf{l}/2) + \Phi_n^2(\mathbf{p} + \mathbf{l}/2) + \Phi_x^2(\mathbf{p} + \mathbf{l}/2) \right], \\ \mathcal{A}^{(b)} &= \frac{1}{1 + \xi/2} \int \frac{d^3 \mathbf{p} d^3 \mathbf{l}}{(2\pi)^6} \left(G(\mathbf{p}, \mathbf{l}) - G_{\text{st}}(\mathbf{l}) \right) \\ &\quad \times \left[\Phi_p(\mathbf{p} + \mathbf{l}/2) \Phi_n(\mathbf{p} - \mathbf{l}/2) + \Phi_n(\mathbf{p} + \mathbf{l}/2) \Phi_p(\mathbf{p} - \mathbf{l}/2) - \Phi_x(\mathbf{p} + \mathbf{l}/2) \Phi_x(\mathbf{p} - \mathbf{l}/2) \right], \\ \mathcal{A}^{(c)} &= \frac{1}{1 + \xi/2} \int \frac{d^3 \mathbf{p} d^3 \mathbf{l} d^3 \mathbf{q}}{(2\pi)^9} G(\mathbf{p}, \mathbf{l}) \left(\frac{\xi}{8\pi m_N} M_{NN}(\mathbf{p}, \mathbf{q}, \mathbf{l}) \right) G(\mathbf{q}, \mathbf{l}) \\ &\quad \times \left[\Phi_p(\mathbf{p} + \mathbf{l}/2) + \Phi_n(\mathbf{p} + \mathbf{l}/2) \right] \left[\Phi_p(\mathbf{q} + \mathbf{l}/2) + \Phi_n(\mathbf{q} + \mathbf{l}/2) \right], \end{aligned} \quad (12)$$

and the different Green functions corresponding to the intermediate $\bar{K}NN$ state read

$$G_{\text{st}}(\mathbf{l}) = \frac{4\pi}{\mathbf{l}^2}, \quad G(\mathbf{p}, \mathbf{l}) = \frac{4\pi}{\mathbf{l}^2(1 + \xi/2) + 2\xi(\mathbf{p}^2 + \gamma^2)}, \quad G_{\text{r}}(\mathbf{p}, \mathbf{l}) = G(\mathbf{p}, \mathbf{l}) - \frac{1}{1 + \xi} G_{\text{st}}(\mathbf{l}). \quad (13)$$

The nucleon-nucleon amplitude M_{NN} which enters $\mathcal{A}^{(c)}$ is determined from a solution of the Lippmann-Schwinger equation for a given two-nucleon potential V_{NN}

$$M_{NN}(\mathbf{p}, \mathbf{q}, \mathbf{l}) = V_{NN}(\mathbf{p}, \mathbf{q}) + \frac{\xi}{2m_N} \int \frac{d^3 \mathbf{k}}{(2\pi)^3} \frac{V_{NN}(\mathbf{p}, \mathbf{k}) M_{NN}(\mathbf{k}, \mathbf{q}, \mathbf{l})}{\mathbf{l}^2(1 + \xi/2) + 2\xi(\mathbf{k}^2 + \gamma^2)}, \quad (14)$$

where we used explicitly that the energy relevant for the study is $E = -\varepsilon_d - \mathbf{l}^2(1 + \xi/2)/2m_K$. Further, the quantity $\Phi_i(\mathbf{q})$ ($i = p, n, x$) represents the convolution of the deuteron wave function $\Psi(r)$ with the re-summed static amplitudes A_i

$$\Phi_i(\mathbf{q}) = \int d^3 \mathbf{r} e^{i\mathbf{q}\mathbf{r}} \Psi(r) A_i(r). \quad (15)$$

The amplitudes $A_i(r)$ obey the system of algebraic equations in the r -space (see e.g. [32])

$$\begin{aligned} A_p &= \tilde{a}_p + \frac{\tilde{a}_p}{r} A_n - \frac{\tilde{a}_x}{r} A_x, \\ A_n &= \tilde{a}_n + \frac{\tilde{a}_n}{r} A_p, \\ A_x &= \tilde{a}_x + \frac{\tilde{a}_x}{r} A_n - \frac{\tilde{a}_u}{r} A_x, \end{aligned} \quad (16)$$

where A_p , A_n and A_x are the amplitudes, in which the last (or the first) interaction of K^- takes place on the proton ($K^-p \rightarrow K^-p$), on the neutron ($K^-n \rightarrow K^-n$) or is of the charge-exchange-type ($K^-p \rightarrow \bar{K}^0n$). The solution of this system yields the required amplitudes

$$A_p = \frac{\tilde{a}_p + \frac{\tilde{a}_p \tilde{a}_n - b_x^2}{r} - \frac{\tilde{a}_n b_x^2}{r^2}}{1 - \frac{\tilde{a}_p \tilde{a}_n}{r^2} + \frac{\tilde{a}_n b_x^2}{r^3}}, \quad A_n = \frac{\tilde{a}_n + \frac{\tilde{a}_p \tilde{a}_n}{r} - \frac{\tilde{a}_n b_x^2}{r^2}}{1 - \frac{\tilde{a}_p \tilde{a}_n}{r^2} + \frac{\tilde{a}_n b_x^2}{r^3}}, \quad A_x = \frac{\tilde{a}_x \left(1 + \frac{\tilde{a}_n}{r}\right)}{1 - \frac{\tilde{a}_p \tilde{a}_n}{r^2} + \frac{\tilde{a}_n b_x^2}{r^3}} \frac{1}{1 + \frac{\tilde{a}_u}{r}}. \quad (17)$$

Here, the quantity b_x is defined in Eq. (4). It is straightforward to see that if one does the replacement $A_i \rightarrow \tilde{a}_i$, the expressions (12) transform exactly to those derived in Ref. [36] for the double scattering diagrams. Note that the symmetric combination $A_p + A_n$ represents the isoscalar contribution to the $\bar{K}NN - \bar{K}NN$ operator which does not change the isospin state of the NN -pair. Being convoluted with the deuteron wave functions in the initial and final states, it yields the static amplitude (2) of $\bar{K}d$ scattering. Similarly, the antisymmetric combination of the amplitudes $A_p - A_n$ as well as the charge exchange amplitude A_x represent the isovector contributions to the $\bar{K}NN - \bar{K}NN$ operator. When applied to the initial deuteron state, these operators give rise to the isospin-1 NN -pair. Following Refs. [36, 38], we therefore decompose the results (12) into the contributions corresponding to the two-nucleon intermediate states with a certain isospin

$$\mathcal{A}^{(1)} = \mathcal{A}^{(a)} + \mathcal{A}^{(b)} + \mathcal{A}^{(c)} = \left\{ \mathcal{A}_1 + \Delta \mathcal{A}_{\text{st},1} \right\} + \left\{ \mathcal{A}_0 + \mathcal{A}^{(c)} + \Delta \mathcal{A}_{\text{st},0} \right\}, \quad (18)$$

where the expression in the first curly bracket in the r.h.s. of Eq. (18) corresponds to the $I = 1$ NN intermediate state while that in the second bracket corresponds to $I = 0$. In order to obtain Eq. (18), the expressions for $\mathcal{A}^{(a)}$ and $\mathcal{A}^{(b)}$ were rewritten using the following rules:

1. The combinations of the functions Φ_i (cf. Eq. (15)) which enter the expressions for $\mathcal{A}^{(a)}$ and $\mathcal{A}^{(b)}$ can be decomposed into the isoscalar and isovector parts using the relations

$$\begin{aligned} \Phi_{p1}^2 + \Phi_{n1}^2 + \Phi_{x1}^2 &= \frac{1}{2} (\Phi_{p1} + \Phi_{n1}) (\Phi_{p1} + \Phi_{n1}) + \frac{1}{2} (\Phi_{p1} - \Phi_{n1}) (\Phi_{p1} - \Phi_{n1}) + \Phi_{x1}^2, \\ \Phi_{p1} \Phi_{n2} + \Phi_{n1} \Phi_{p2} - \Phi_{x1} \Phi_{x2} &= \frac{1}{2} (\Phi_{p1} + \Phi_{n1}) (\Phi_{p2} + \Phi_{n2}) - \frac{1}{2} (\Phi_{p1} - \Phi_{n1}) (\Phi_{p2} - \Phi_{n2}) - \Phi_{x1} \Phi_{x2}. \end{aligned}$$

where the second subscript indicates that the functions Φ in Eq. (12) depend on two different momenta $\mathbf{l}_1 = \mathbf{p} + \mathbf{l}/2$ and $\mathbf{l}_2 = \mathbf{p} - \mathbf{l}/2$, respectively. Since the Φ_i are proportional to the A_i , the first term in the r.h.s of these equations contributes to $I = 0$ NN intermediate state while the others correspond to $I = 1$. Using these relations one determines the resulting $I = 0$ and $I = 1$ contributions in the curly brackets of Eq. (18).

2. It appears useful to further decompose the net $I = 0$ and $I = 1$ contributions in such a way that the terms \mathcal{A}_0 and \mathcal{A}_1 contain the same renormalized $\bar{K}NN$ Green function G_r (see Eq. (13)). The trivial corrections $\Delta \mathcal{A}_{\text{st},0}$ and $\Delta \mathcal{A}_{\text{st},1}$, which can be expanded into the integer powers of ξ , appear as the result of this separation as well.

Thus, one gets

$$\begin{aligned}
\mathcal{A}_0 &= \frac{1}{2} \frac{1}{1 + \xi/2} \int \frac{d^3 \mathbf{p} d^3 \mathbf{l}}{(2\pi)^6} [\Phi_p(\mathbf{l}_1) + \Phi_n(\mathbf{l}_1)] G_r(\mathbf{p}, \mathbf{l}) [\Phi_p(\mathbf{l}_1) + \Phi_n(\mathbf{l}_1) + \Phi_p(\mathbf{l}_2) + \Phi_n(\mathbf{l}_2)] , \\
\mathcal{A}_1 &= \frac{1}{2} \frac{1}{1 + \xi/2} \int \frac{d^3 \mathbf{p} d^3 \mathbf{l}}{(2\pi)^6} G_r(\mathbf{p}, \mathbf{l}) \\
&\quad \times \left[(\Phi_p(\mathbf{l}_1) - \Phi_n(\mathbf{l}_1)) (\Phi_p(\mathbf{l}_1) - \Phi_n(\mathbf{l}_1) - \Phi_p(\mathbf{l}_2) + \Phi_n(\mathbf{l}_2)) + 2\Phi_x(\mathbf{l}_1) (\Phi_x(\mathbf{l}_1) - \Phi_x(\mathbf{l}_2)) \right] ,
\end{aligned} \tag{19}$$

and

$$\begin{aligned}
\Delta \mathcal{A}_{\text{st},0} &= - \frac{\xi}{2(1 + \xi)(1 + \xi/2)} \int d^3 \mathbf{r} \frac{\Psi^2(\mathbf{r})}{r} (A_p(r) + A_n(r))^2 , \\
\Delta \mathcal{A}_{\text{st},1} &= \frac{\xi}{2(1 + \xi)(1 + \xi/2)} \int d^3 \mathbf{r} \frac{\Psi^2(\mathbf{r})}{r} ((A_p(r) - A_n(r))^2 + 2A_x(r)^2) .
\end{aligned} \tag{20}$$

The expressions written in the isospin basis allow for a very clear physical interpretation of the cancellations between various individual recoil corrections, as will be discussed in section 4.2.

4. Perturbative expansion of the first-order correction in powers of ξ

4.1. Formalism

The expression of the single recoil insertion, which was given in the previous section, depends on the variable ξ in a non-trivial way. In order to establish systematic power-counting rules, it is therefore necessary to perform an expansion of this expression in ξ . Further, considering such an expansion helps one to reveal the pattern of cancellations of the leading terms, which has been discussed already in Ref. [36]. Note that these cancellations are crucial for discussing the convergence of the perturbative method, which is described in the present paper. Note also that the final *numerical* results presented in section 5 include the *full* expression of the one recoil insertion and do not rely on this expansion.

As already shown in Ref. [36], the $\bar{K}d$ scattering length can be systematically expanded in the half-integer powers of ξ . As an illustrative example, the expansion of the double scattering diagrams was performed, and a relatively rapid convergence was observed. In this paper, we investigate the convergence of this expansion for the case of multiple scattering series with one recoil insertion.

Below, we shall use the uniform expansion method, see Refs. [39, 40]. In this method, different momentum regions are identified, according to the scales appearing in the problem. The integrand is expanded in each region before performing the integration, and the results are summed up. In our case, the relevant regions are defined by two momentum scales in the full $\bar{K}NN$ Green function (13). One therefore finds three relevant integration regions:

1) low-momentum region:

The internal kaon momentum l is much smaller than the typical deuteron scale $p \sim \langle 1/r \rangle \sim m_\pi$, but still of the same order of magnitude as $\sqrt{\xi}p$. In this region, the Green function $G(\mathbf{p}, \mathbf{l})$ “feels” the presence of the nearby 3-body singularity. Meanwhile, all other quantities, such as the functions $\Phi_i(\mathbf{p} \pm \mathbf{l}/2)$, can be systematically expanded, assuming $l \ll p$. Given that $l \sim \sqrt{\xi}p$, non-integer orders of ξ emerge after the integration.

2) high-momentum region:

In this region, $l \sim p$ and all retarded terms in $G(\mathbf{p}, \mathbf{l})$ are suppressed by ξ . The direct expansion in ξ leads to the appearance of integer orders in the expansion.

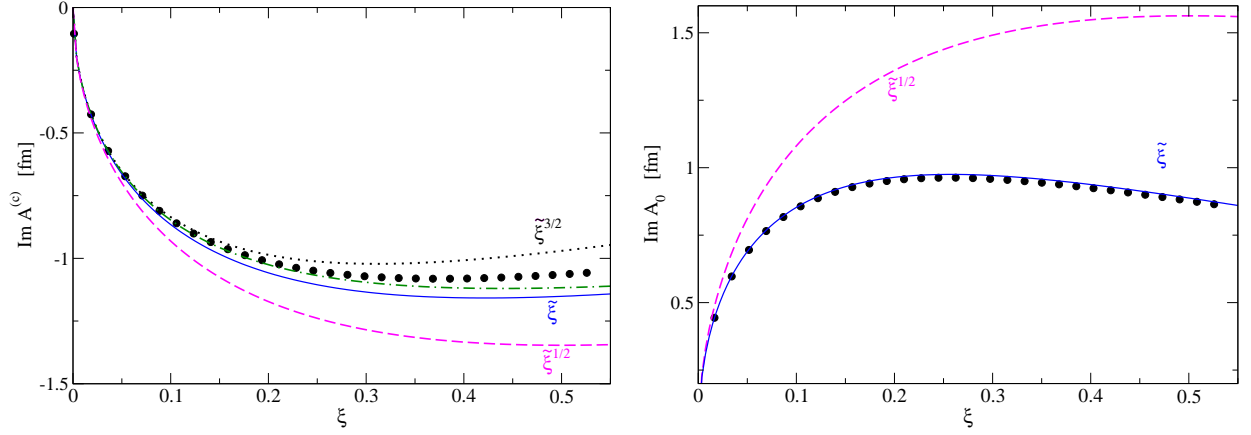


Figure 3: Expansion of the amplitude \mathcal{A}_0 and $\mathcal{A}^{(c)}$ in powers of $\tilde{\xi} = \xi/(1 + \xi/2)$: left panel – $\text{Im } \mathcal{A}^{(c)}$, right panel – $\text{Im } \mathcal{A}_0$. Dashed, solid, dotted, and dot-dashed lines correspond to the expansion up to the order $\tilde{\xi}^{1/2}$, $\tilde{\xi}$, $\tilde{\xi}^{3/2}$, and $\tilde{\xi}^2$, respectively. The result of the full calculation is presented by the black dots.

3) intermediate region:

The momenta in the intermediate region obey $\sqrt{\xi}p \ll l \ll p$. The integrand in this region can be obtained, if one applies the low-momentum expansion to the integrand already expanded in the high-momentum region or vice versa.

The original integrand (I) of the amplitude can then be written as

$$I = I_{\text{low}} + I_{\text{high}} - I_{\text{interm}}. \quad (21)$$

Evaluating the integral over the whole momentum range, we obtain the amplitudes at a given order in ξ . Note that the integrand, being expanded in the regions 1) and 2), contains ultraviolet- as well as infrared-divergent terms. However, these divergences cancel exactly with those that emerge from the intermediate region, rendering the result finite and independent of the regularization scheme.

4.2. Leading-order recoil correction

It has been known for many years that, due to the emerging cancellations, the recoil corrections to pion-deuteron scattering at threshold are smaller than one would naively expect, see, e.g., Refs. [41–43]. In the isovector channel, relevant for πd scattering, the mechanism behind this cancellation was identified in Ref. [38], see also Refs. [23, 44] for further discussions. In Ref. [36], the arguments were summarized and generalized to the isoscalar channel which is of importance for $\bar{K}d$ scattering. In all these studies, however, the recoil effect was studied for the double-scattering process only that is fully justified for πd scattering but does not suffice for $\bar{K}d$ scattering. Here we discuss, what happens with the leading $O(\xi^{1/2})$ correction in the presence of the static multiple-scattering ladders. If this correction survives, it would give an estimated 70% correction to \mathcal{A} , in contradiction to a relatively good agreement between the static MSS and Faddeev calculations.

The origin of the cancellation of the leading isovector correction in the quantity \mathcal{A}_1 from Eq. (19) lies in the fact that the NN pair with total isospin $I = 1$ must have orbital momentum $L = 1$, as a consequence of the Pauli selection rules. Hence, the diagram c in Fig. 2, which accounts for the S-wave NN interaction, does not contribute in this case. Meanwhile, the diagrams a and b do produce $O(\xi^{1/2})$ corrections individually. Those, however, correspond to the NN states in the S-wave and thus naturally cancel in the sum. This can be seen immediately since, as argued above, all corrections with the non-integer powers of ξ emerge from the low-momentum region. Expanding then the integrand in Eq. (19) in the assumption $l \ll p$, one immediately finds that the leading contribution to \mathcal{A}_1 vanishes.

On the contrary, in the isoscalar case, the NN intermediate states can appear in the S-wave. This means that all diagrams in Fig. 2 are relevant. Furthermore, for the isoscalar $\bar{K}N$ -interaction, the quantum numbers of the intermediate NN pair must coincide with those of the deuteron, i.e. the NN state appears in the 3S_1 partial wave. It was shown in Ref. [36] that the sum of the diagrams of type shown in Fig. 2 gives the full Green function of the

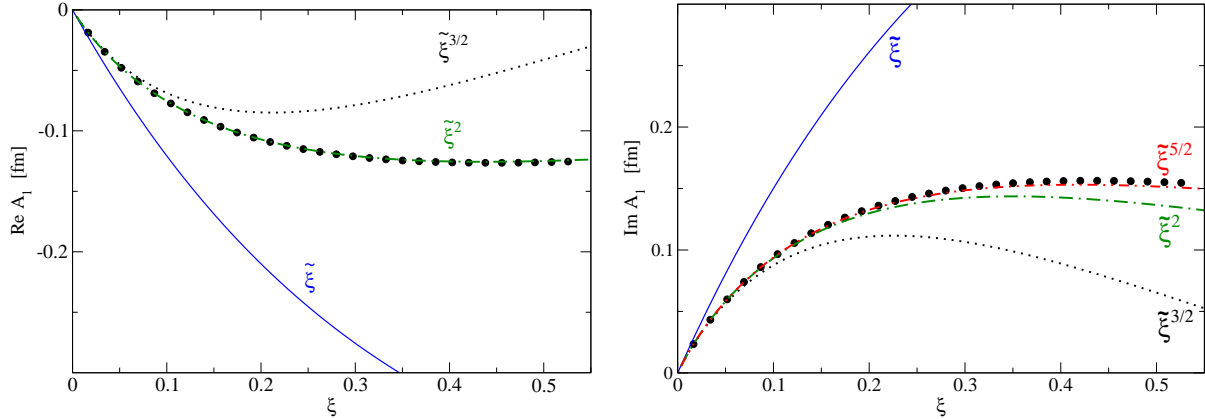


Figure 4: Expansion of the amplitude \mathcal{A}_1 in powers of $\tilde{\xi} = \xi/(1 + \xi/2)$: left panel – $\text{Re } \mathcal{A}_1$, right panel – $\text{Im } \mathcal{A}_1$. Solid, dotted, dot-dashed and double-dot-dashed lines correspond to the expansion up to the order $\tilde{\xi}$, $\tilde{\xi}^{3/2}$, $\tilde{\xi}^2$, $\tilde{\xi}^{5/2}$, respectively. The result of the full calculation is presented by the black dots.

NN state, which should be orthogonal to the bound-state deuteron wave function due to the completeness condition. This was the origin of cancellation of the isoscalar recoil corrections in the double-scattering diagrams, considered in Ref. [36]. The situation is, however, different in the multiple-scattering case, since the infinite static ladders (see the shaded blocks in Fig. 2) separate the bound-state and continuum wave functions, providing the effect of screening. Therefore, the cancellation of the isoscalar $O(\xi^{1/2})$ recoil correction is not exact, although it is still largely present, as will be shown below.

4.3. Convergence of the expansion in ξ

In Fig. 3 we demonstrate the convergence of the expansion for the isoscalar case. The Hulthén NN potential is used in the calculations³. Note further that we found it useful to introduce a modified expansion parameter $\tilde{\xi} = \xi/(1 + \xi/2)$. The convergence of the series in this new parameter improves substantially, see Appendix A for the explicit expressions. For illustrative purposes, we present the results for $\text{Im } \mathcal{A}_0$ and $\text{Im } \mathcal{A}^{(c)}$ separately, both dominated by the leading order $O(\tilde{\xi}^{1/2})$ terms. Meanwhile, these corrections appear with different signs and thus largely cancel in the sum. It is interesting that already at the order $\tilde{\xi}$, the expanded results nicely agree with the exact ones. Analogous results for the isovector case are shown in Fig. 4 for $\text{Re } \mathcal{A}_1$ (left panel) and $\text{Im } \mathcal{A}_1$ (right panel). In this case, the expansion starts from the order $\tilde{\xi}$, in accordance with the Pauli selection rules. The expansion in half-integer powers of $\tilde{\xi}$ for the isovector case converges a little slower than for the isoscalar one, but still provides a very good approximation to the unexpanded results already at the order $\tilde{\xi}^2$.

5. Numerical results for the $\bar{K}d$ scattering length

5.1. The role of recoil effects for kaonic deuterium

We are now in the position to analyze the role of the recoil corrections in the $\bar{K}d$ scattering length. The results of our calculations for one recoil insertion are given in Table 1. As already mentioned, at this stage, we use the phenomenological nucleon-nucleon separable potentials instead of the more complicated potentials, constructed within the chiral EFT. In particular, the results of the calculations shown in Table 1 are obtained for the Hulthén and PEST NN potentials, see Appendix B. The following values of the $\bar{K}N$ scattering lengths are used as an input [28]:

$$a_0 = (-1.62 + i0.78) \text{ fm}, \quad a_1 = (0.18 + i0.68) \text{ fm}, \quad (22)$$

The following conclusions can be drawn, based on the results shown in Table 1:

³This potential is regular at short distances (does not depend on the large mass scales). Consequently, there is no need for introducing a short-distance regularization that simplifies the calculation substantially.

Hulthén potential			PEST potential		
\mathcal{A}_{st}	$-1.49 + i1.19$		\mathcal{A}_{st}	$-1.55 + i1.25$	
$\mathcal{A}^{(1)}$	\mathcal{A}_1	$-0.13 + i0.16$	$\mathcal{A}^{(1)}$	\mathcal{A}_1	$-0.13 + i0.18$
	$\Delta\mathcal{A}_{\text{st},1}$	$+0.12 - i0.20$		$\Delta\mathcal{A}_{\text{st},1}$	$+0.13 - i0.22$
		$+0.00 - i0.04$			$+0.00 - i0.04$
	\mathcal{A}_0	$-0.27 + i0.87$		\mathcal{A}_0	$-0.29 + i0.97$
	$\Delta\mathcal{A}_{\text{st},0}$	$-0.12 + i0.33$		$\Delta\mathcal{A}_{\text{st},0}$	$-0.11 + i0.34$
	$\mathcal{A}^{(c)}$	$+0.35 - i1.06$		$\mathcal{A}^{(c)}$	$+0.36 - i1.19$
		$-0.03 + i0.13$			$-0.04 + i0.12$
	Sum:	$-0.03 + i0.09$		Sum:	$-0.04 + i0.08$
$\mathcal{A}_{\text{st}} + \mathcal{A}^{(1)}$	$-1.52 + i1.27$		$\mathcal{A}_{\text{st}} + \mathcal{A}^{(1)}$	$-1.59 + i1.32$	

Table 1: The recoil corrections to the $\bar{K}d$ scattering length from one insertion of the retarded block. All quantities are given in units of fm.

- i) In the isoscalar channel, the individual contributions, which still contain the dominant $O(\tilde{\xi}^{1/2})$ term, are very large, especially the imaginary parts thereof. However, they undergo significant cancellations, yielding only about a 10% net correction to the imaginary part of the static term.
- ii) The resulting isovector recoil correction appears to be even smaller providing only about a 3% correction to the static term. Its smallness can be understood from the exact cancellation of the $O(\tilde{\xi}^{1/2})$ term along with some additional cancellations among higher-order terms. This effect was already discussed in Ref. [36], see also Fig. 4.
- iii) The recoil contributions $\Delta\mathcal{A}_{\text{st},0}$ and $\Delta\mathcal{A}_{\text{st},1}$, which start to contribute at the order $\tilde{\xi}$, are still sizable. These are, however, largely canceled by other contributions, pointing at cancellations that emerge at this and higher orders in $\tilde{\xi}$. At this stage, the mechanism of such cancellations is unclear and needs to be addressed.
- iv) The net correction $\mathcal{A}^{(1)}$ which stems from one recoil insertion in the MS diagrams appears to be quite small, of order of $\simeq 6 - 8\%$ of \mathcal{A}_{st} , despite the large value of ξ . An additional suppression is partly accounted for by cancellations of the isoscalar and isovector recoil corrections.
- v) Ref. [28] gives the value of the $\bar{K}d$ scattering length, obtained by the solution of the Faddeev equations with the one-channel energy-independent optical potential. The parameters of this potential were adjusted to reproduce the scattering lengths (22). The calculation, carried in Ref. [28], yields $\mathcal{A} \simeq (-1.47 + 1.11i)$ fm, see the half-empty square in Fig. 12 in that paper.

Although the input in the two calculations might still differ in several aspects, such as different NN models, or the use of the off-shell form factors, needed to regularize the Faddeev calculations, it is instructive to compare this result with the pertinent results shown in Table 1. In particular, one can see that the differences between the static result and the solution of the Faddeev equation are, generally, of the same order as the full recoil correction $\mathcal{A}^{(1)}$.

Finally, few words should be said about the higher-order recoil corrections (two or more recoil insertions). Albeit the results with one insertion look encouraging, these do not completely guarantee the convergence of the procedure, since the smallness of the first-order correction could still follow from some peculiar cancellations. In this respect, according to the above discussion, the study of the corrections to the *isoscalar* amplitude, where the cancellation of the leading $O(\tilde{\xi}^{1/2})$ terms is not complete due to the presence of the static ladders, appears to be crucial.

5.2. Prediction for the $\bar{K}d$ scattering length

In this paper, we developed an EFT framework which directly relates the $\bar{K}N$ scattering lengths to the $\bar{K}d$ scattering length. Since the latter is not yet measured in the experiment, we find it useful to predict in which region this quantity

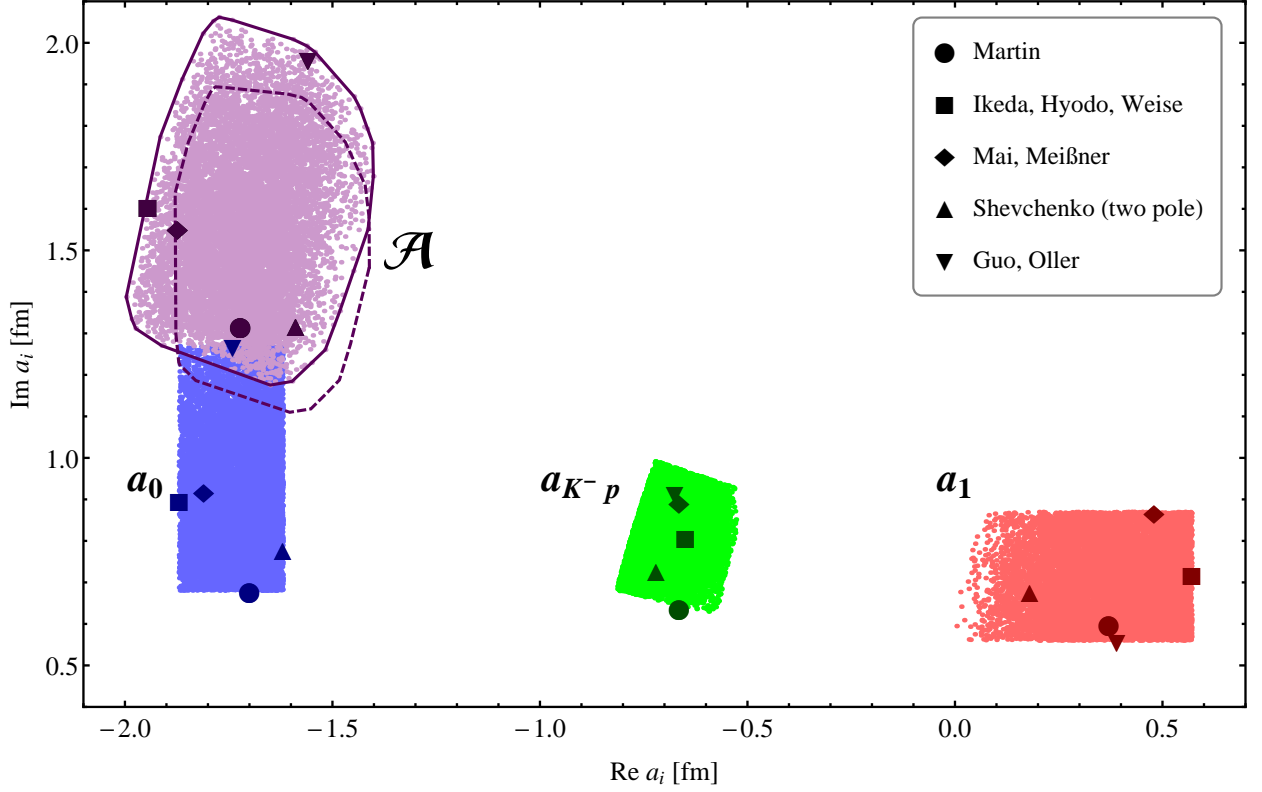


Figure 5: The antikaon-deuteron scattering length \mathcal{A} (purple dots) for given input values of the antikaon-nucleon scattering lengths a_0 (blue) and a_1 (red). These lengths are chosen to be randomly distributed in the rectangular areas, restricted by results from the SIDDHARTA experiment [12], see Eq. (23). The full purple line shows the convex hull of all results for the $\bar{K}d$ scattering length, whereas the purple dashed line is the convex hull for the static results (not shown explicitly).

could lie for various input values of the $\bar{K}N$ scattering lengths, known from the literature. This procedure allows us to test the sensitivity of the final outcome to the input and, what is not less important, the sensitivity of the recoil correction to the same input.

We have adopted the following strategy. We assume that the NN interaction is described by the PEST potential [45] and examine a broad variety of the models for the $\bar{K}N$ interaction. Some of the models are listed in Table 2. For each of the models, using the quoted values of the $\bar{K}N$ scattering lengths a_0 and a_1 , we calculate the $\bar{K}d$ scattering length in the static approximation, as well as including the first-order recoil correction. The results are presented in Fig. 5.

Moreover, in order to minimize the dependence on the input, we randomly generate $\bar{K}N$ scattering lengths from the rectangular areas

$$-1.87 \leq \text{Re } a_0 \leq -1.62, \quad +0.68 \leq \text{Im } a_0 \leq +1.27, \quad -0.06 \leq \text{Re } a_1 \leq +0.57, \quad +0.56 \leq \text{Im } a_1 \leq +0.87. \quad (23)$$

These intervals include most values of a_0 and a_1 , known in the literature. Further, for each random pair a_0 and a_1 we check that $a_p = (a_0 + a_1)/2$ obeys the constraints⁴ imposed by the SIDDHARTA experiment [12] and reject the pairs for which this constraint is not fulfilled. Again, we calculate the $\bar{K}d$ scattering length in the static approximation, as well as with first-order recoil correction. The dotted and solid curves in Fig. 5 show the convex hulls for the results of these calculations, determining the region where the measured value of the $\bar{K}d$ scattering length is expected to lie.

Several important observations can be made from Table 2 and Fig. 5. First of all, the $\bar{K}d$ scattering length turns out to be quite sensitive to the input values of a_0 and a_1 . Moreover, albeit non-negligible, the first-order recoil correction

⁴Here, for consistency reasons, we have neglected the isospin-breaking effects in the quantity a_p . These effects might become substantial, see Ref. [16].

Reference	a_0 [fm]	a_1 [fm]	\mathcal{A}_{st} [fm]	$\mathcal{A} = \mathcal{A}_{\text{st}} + \mathcal{A}^{(1)}$ [fm]
Martin [46]	$-1.70 + i0.68$	$+0.37 + i0.60$	$-1.65 + i1.23$	$-1.72 + i1.32$
Ikeda, Hyodo, Weise [9]	$-1.87 + i0.90$	$+0.57 + i0.72$	$-1.87 + i1.48$	$-1.95 + i1.61$
Mai, Meißner [10]	$-1.81 + i0.92$	$+0.48 + i0.87$	$-1.82 + i1.45$	$-1.87 + i1.56$
Shevchenko (two pole) [29]	$-1.62 + i0.78$	$+0.18 + i0.68$	$-1.55 + i1.25$	$-1.59 + i1.32$
Guo, Oller [47]	$-1.74 + i1.27$	$+0.39 + i0.56$	$-1.58 + i1.83$	$-1.56 + i1.96$
Borasoy, Meißner, Nißler [6]	$-1.64 + i0.75$	$-0.06 + i0.57$	$-1.49 + i1.12$	$-1.53 + i1.18$

Table 2: The $\bar{K}d$ scattering length for different input values of the $\bar{K}N$ scattering lengths.

seems to be moderate for very different input values of a_0 and a_1 . These two observations lead us to the conclusion that rather stringent constraints on a_0 and a_1 would emerge, once the $\bar{K}d$ scattering length is measured at a reasonable accuracy.

6. Conclusions

- i) In this paper we have studied the first-order recoil correction in the multiple-scattering series for the $\bar{K}d$ scattering length. The static $\bar{K}N$ interactions are treated non-perturbatively and are summed up to all orders. A perturbative framework is set up for the calculation of the higher-order recoil corrections (two and more insertions). We plan to address this issue in our forthcoming publication.
- ii) The main message which we would like to convey to the reader is that the recoil corrections, which, given the large value of the parameter $\xi \simeq 0.5$, were *a priori* expected to be very large, are in fact rather moderate. This conclusion is quite robust and holds for all input values of a_0, a_1 , randomly taken from the literature. The smallness of the recoil corrections can, in part, be attributed to large cancellations of the leading contributions in the expansion in ξ , which were discussed above in detail. Partial cancellations could be occurring in the sub-leading contributions as well. This issue, however, requires further investigation.
- iii) The investigation of the first-order recoil corrections is only the first step towards the development of a systematic EFT framework for the low-energy $\bar{K}d$ system. The next steps would include, in particular, estimation of the size of higher-order recoil corrections and a careful investigation of convergence of the perturbative approach; a study of the role of the $\Lambda(1405)$ resonance in the $\bar{K}d$ scattering; a systematic inclusion of higher-order terms in the effective Lagrangian such as e.g. the effective range; employing the NN potentials obtained in chiral EFT instead of the phenomenological models and a systematic inclusion of isospin-breaking effects. These studies would provide important steps towards a consistent theory of the low-energy $\bar{K}d$ system which is necessary in order to analyze forthcoming data on the kaonic deuterium atom [19, 20].

Acknowledgement The authors would like to thank A. Cieply, Ulf-G. Meißner, A. Gal and W. Weise for useful discussions. We are thankful to Ulf-G. Meißner for a careful reading of the manuscript. This work is partly supported by the EU Integrated Infrastructure Initiative HadronPhysics3 Project under Grant Agreement no. 283286. We also acknowledge the support by the DFG and NSFC (CRC 110, “Symmetries and the Emergence of Structure in QCD”). One of the authors (AR) acknowledges the support by the Shota Rustaveli National Science Foundation (Project DI/13/02) and by Volkswagenstiftung under contract no. 86260.

Appendix A. Expansion of the individual amplitudes in powers of ξ

In this appendix, we discuss the expansion of the amplitudes $\mathcal{A}_0, \mathcal{A}_1$ and $\mathcal{A}^{(c)}$ in powers of ξ . Since the Green function, entering the expression for these amplitudes, can be written in the following form

$$G(\mathbf{p}, \mathbf{l}) = \frac{4\pi}{1 + \xi/2} \frac{1}{\mathbf{l}^2 + 2\tilde{\xi}(\mathbf{p}^2 + \gamma^2)}, \quad \tilde{\xi} = \frac{\xi}{1 + \xi/2} = O(\xi), \quad (\text{A.1})$$

one may argue that the quantity $\tilde{\xi}$ is an appropriate expansion parameter. Namely, in the high-energy region we have $l \simeq p$ and the function $G(\mathbf{p}, \mathbf{l})$ should be Taylor-expanded in the momentum \mathbf{p} . On the opposite, in the low-energy region $l \simeq \tilde{\xi}^{1/2} p$, the function $G(\mathbf{p}, \mathbf{l})$ stays intact, whereas other parts of the integrand – namely, the wave functions and the NN amplitude – are Taylor-expanded in the momentum \mathbf{l} . It can be easily checked that the convergence of the series in $\tilde{\xi}$ is substantially better than in ξ , since the latter series contains oscillating terms that emerge from expanding $\tilde{\xi} = \xi/(1 + \xi/2)$ in powers of ξ .

Since the integrals we are dealing with are convergent, we are free to choose the regularization scheme. Using dimensional regularization, it can be easily shown that the expansion of \mathcal{A}_0 and \mathcal{A}_1 reads

$$\mathcal{A}_i = \frac{8\pi}{(1 + \xi/2)^2} \left(\sum_{n=1}^{\infty} B_i^n \tilde{\xi}^n + \sum_{n=0}^{\infty} D_i^n \tilde{\xi}^{\frac{2n+1}{2}} \right), \quad (\text{A.2})$$

where $(i = 0, 1)$ and

$$\begin{aligned} B_i^n &= \frac{(-1)^n}{4} \int \frac{d^3 \mathbf{p} d^3 \mathbf{l}}{(2\pi)^6} \frac{1}{\mathbf{l}^2} \left(\frac{(2(\mathbf{p}^2 + \gamma^2))^n}{\mathbf{l}^{2n}} - \frac{1}{2^n} \right) \Phi_i(\mathbf{p}, \mathbf{l}) \\ D_i^n &= \frac{(-1)^{n+1}}{4} \int \frac{d^3 \mathbf{p}}{(2\pi)^3} \frac{1}{4\pi} (2(\mathbf{p}^2 + \gamma^2))^{\frac{2n+1}{2}} \Phi_i^{(2n)}(\mathbf{p}). \end{aligned} \quad (\text{A.3})$$

Here the functions $\Phi_i(\mathbf{p}, \mathbf{l})$ are defined as

$$\begin{aligned} \Phi_0(\mathbf{p}, \mathbf{l}) &= \left(\Phi_p(\mathbf{l}_1) + \Phi_n(\mathbf{l}_1) \right) \left(\Phi_p(\mathbf{l}_1) + \Phi_n(\mathbf{l}_1) + \Phi_p(\mathbf{l}_2) + \Phi_n(\mathbf{l}_2) \right), \\ \Phi_1(\mathbf{p}, \mathbf{l}) &= \left(\Phi_p(\mathbf{l}_1) - \Phi_n(\mathbf{l}_1) \right) \left(\Phi_p(\mathbf{l}_1) - \Phi_n(\mathbf{l}_1) - \Phi_p(\mathbf{l}_2) + \Phi_n(\mathbf{l}_2) \right) + 2\Phi_x(\mathbf{l}_1) (\Phi_x(\mathbf{l}_1) - \Phi_x(\mathbf{l}_2)). \end{aligned} \quad (\text{A.4})$$

These functions can be Taylor-expanded as

$$\Phi_i(\mathbf{p}, \mathbf{l}) = \sum_{n=0}^{\infty} \frac{\mathbf{l}^{2n}}{(2n+1)2n!} \Delta_l^n \Phi_i(\mathbf{p}, \mathbf{l}) \Big|_{\mathbf{l}=0} \doteq \sum_{n=0}^{\infty} \mathbf{l}^{2n} \Phi_i^{(2n)}(\mathbf{p}). \quad (\text{A.5})$$

Similarly, the expansion of $\mathcal{A}^{(c)}$ reads:

$$\mathcal{A}^{(c)} = \frac{8\pi}{(1 + \xi/2)^2} \left(\sum_{n=1}^{\infty} B_c^n \tilde{\xi}^n + \sum_{n=0}^{\infty} D_c^n \tilde{\xi}^{\frac{2n+1}{2}} \right). \quad (\text{A.6})$$

In general, explicit expressions for the coefficients B_c, D_c are very complicated. These, however, simplify somewhat, when the potential V_{NN} is separable. Below, we give the expressions for the first few coefficients in case of the Hulthén potential, defined in Appendix B

$$\begin{aligned} B_c^1 &= \frac{1}{4m_N} \int \frac{d^3 \mathbf{p} d^3 \mathbf{q} d^3 \mathbf{l}}{(2\pi)^9} \frac{\Phi_c(\mathbf{p}, \mathbf{q}, \mathbf{l})}{\mathbf{l}^4} V_{NN}(\mathbf{p}, \mathbf{q}), \\ B_c^2 &= \frac{1}{4m_N} \int \frac{d^3 \mathbf{p} d^3 \mathbf{q} d^3 \mathbf{l}}{(2\pi)^9} \frac{\Phi_c(\mathbf{p}, \mathbf{q}, \mathbf{l})}{\mathbf{l}^6} V_{NN}(\mathbf{p}, \mathbf{q}) \left(\frac{\lambda}{16\pi m_N \beta} - 2(\mathbf{p}^2 + \mathbf{q}^2 + 2\gamma^2) \right), \\ D_c^n &= \frac{1}{4m_N} \int \frac{d^3 \mathbf{p} d^3 \mathbf{q} d^3 \mathbf{l}}{(2\pi)^9} \frac{V_{NN}(\mathbf{p}, \mathbf{q})}{1 - A(\mathbf{l})} \frac{\mathbf{l}^{2n} \Phi_c^{(2n)}(\mathbf{p}, \mathbf{q})}{(\mathbf{l}^2 + 2(\mathbf{p}^2 + \gamma^2))(\mathbf{l}^2 + 2(\mathbf{q}^2 + \gamma^2))} \quad \text{for } n = 0, 1. \end{aligned} \quad (\text{A.7})$$

Here, the function $\Phi_c(\mathbf{p}, \mathbf{q}, \mathbf{l})$ is defined as

$$\Phi_c(\mathbf{p}, \mathbf{q}, \mathbf{l}) = \left(\Phi_p(\mathbf{p} + \mathbf{l}/2) + \Phi_n(\mathbf{p} + \mathbf{l}/2) \right) \left(\Phi_p(\mathbf{q} + \mathbf{l}/2) + \Phi_n(\mathbf{q} + \mathbf{l}/2) \right). \quad (\text{A.8})$$

The Taylor expansion of this function at a small \mathbf{l} takes the form

$$\Phi_c(\mathbf{p}, \mathbf{q}, \mathbf{l}) = \sum_{n=0}^{\infty} \frac{\mathbf{l}^{2n}}{(2n+1)2n!} \Delta_l^n \Phi_c(\mathbf{p}, \mathbf{q}, \mathbf{l}) \Big|_{\mathbf{l}=0} \doteq \sum_{n=0}^{\infty} \mathbf{l}^{2n} \Phi_c^{(2n)}(\mathbf{p}, \mathbf{q}). \quad (\text{A.9})$$

Further, the quantity $A(\mathbf{l})$ in (A.7) is defined as

$$A(\mathbf{l}) = \frac{1}{2m_N} \int \frac{d^3\mathbf{q}}{(2\pi)^3} \frac{V_{NN}(\mathbf{q}, \mathbf{q})}{\mathbf{l}^2 + 2(\mathbf{q}^2 + \gamma^2)}. \quad (\text{A.10})$$

Appendix B. Nucleon-Nucleon potentials used in the calculations

In this section, we specify the nucleon-nucleon potentials used in the calculations. For the kaon, nucleon masses and for the deuteron binding energy the following input values have been used:

$$M_K = 493.677 \text{ MeV}, \quad m_N = 938.92 \text{ MeV}, \quad \varepsilon_d = 2.2249 \text{ MeV}. \quad (\text{B.1})$$

Appendix B.1. Hulthén potential

The simplest form of the NN potential assumed in this work is the so-called Hulthén potential. This is a rank-1 separable potential, defined by

$$V_{NN}(\mathbf{p}, \mathbf{q}) = \lambda g(\mathbf{p})g(\mathbf{q}), \quad g(\mathbf{p}) = 1/(\mathbf{p}^2 + \beta^2). \quad (\text{B.2})$$

Here $\beta = 1.4 fm^{-1}$ while $\lambda = 32\pi m_N \beta (\beta + \gamma)^2$ for consistency reasons. In its ansatz it is very similar to the more sophisticated phenomenological potentials, such as given in Refs. [45]. While being less realistic than the latter, it contains only long range physics and is therefore perfectly suited to study some basic properties of our framework, e.g., the expansion in ξ .

Appendix B.2. PEST potential

A more realistic potential is a separable one which is build from the Paris potential (see Ref. [48]) by applying the Ernst-Shakin-Thaler method. This potential is therefore referred to as the PEST potential in Ref. [45]. It practically coincides with the on- and off-shell behaviour of the Paris potential and is given in a fairly simple form:

$$V_{NN}(\mathbf{p}, \mathbf{q}) = -g(\mathbf{p})g(\mathbf{q}), \quad g(\mathbf{p}) = \sum_{i=1}^6 \frac{C_i}{\mathbf{p}^2 + \beta_i^2}, \quad (\text{B.3})$$

where the parameters β_i and C_i are given in the table below. It should also be mentioned that the Lippmann-Schwinger equation, which is used in Ref. [45], has a different normalization than the one in the present paper:

$$(\gamma^2 + \mathbf{p}^2)\Psi(\mathbf{p}) = \frac{m_N}{4\pi} \int d^3\mathbf{q} V_{NN}(\mathbf{p}, \mathbf{q})\Psi(\mathbf{q}). \quad (\text{B.4})$$

	$i = 1$	$i = 2$	$i = 3$	$i = 4$	$i = 5$	$i = 6$
$\beta_i [fm^{-1}]$	1.5	3.0	4.5	6.0	7.5	9.0
$C_i [MeV^{1/2} fm^{-1/2}]$	3.3786469	-637.41908	1750.2432	3561.3535	-12939.749	8656.6202

References

References

- [1] N. Kaiser, P. B. Siegel and W. Weise, Nucl. Phys. A **594** (1995) 325 [arXiv:nucl-th/9505043].
- [2] E. Oset and A. Ramos, Nucl. Phys. A **635** (1998) 99 [arXiv:nucl-th/9711022]; J. A. Oller, E. Oset and A. Ramos, Prog. Part. Nucl. Phys. **45** (2000) 157 [arXiv:hep-ph/0002193];
- [3] J. A. Oller and U.-G. Meißner, Phys. Lett. B **500** (2001) 263 [arXiv:hep-ph/0011146].
- [4] B. Borasoy, R. Nißler and W. Weise, Phys. Rev. Lett. **94** (2005) 213401 [arXiv:hep-ph/0410305]; Eur. Phys. J. A **25** (2005) 79 [arXiv:hep-ph/0505239]; Phys. Rev. Lett. **96** (2006) 199201 [arXiv:hep-ph/0512279].

- [5] J. A. Oller, Eur. Phys. J. A **28** (2006) 63 [arXiv:hep-ph/0603134].
- [6] B. Borasoy, U.-G. Meißner and R. Nisler, Phys. Rev. C **74** (2006) 055201 [arXiv:hep-ph/0606108].
- [7] D. Jido, J. A. Oller, E. Oset, A. Ramos and U.-G. Meißner, Nucl. Phys. A **725** (2003) 181 [arXiv:nucl-th/0303062];
- [8] C. Garcia-Recio, M. F. M. Lutz and J. Nieves, Phys. Lett. B **582** (2004) 49 [arXiv:nucl-th/0305100];
- [9] Y. Ikeda, T. Hyodo and W. Weise, Nucl. Phys. A **881** (2012) 98 [arXiv:1201.6549 [nucl-th]].
- [10] M. Mai and U.-G. Meißner, Nucl. Phys. A **900** (2013) 51 [arXiv:1202.2030 [nucl-th]].
- [11] W. Weise, *Deeply bound meson-nuclear states: Concepts and strategies*, talk given at: EXA05, February 21–25, 2005, Vienna, Austria [arXiv:nucl-th/0507058].
- [12] M. Bazzi, G. Beer, L. Bombelli, A. M. Bragadireanu, M. Cargnelli, G. Corradi, C. Curceanu (Petrascu) and A. d’Uffizi *et al.*, Phys. Lett. B **704** (2011) 113 [arXiv:1105.3090 [nucl-ex]].
- [13] M. Iwasaki *et al.*, Phys. Rev. Lett. **78** (1997) 3067; T. M. Ito *et al.*, Phys. Rev. C **58** (1998) 2366.
- [14] J. Zmeskal *et al.*, Nucl. Phys. A **754** (2005) 369.
- [15] S. Deser, M. L. Goldberger, K. Baumann and W. E. Thirring, Phys. Rev. **96** (1954) 774.
- [16] U.-G. Meißner, U. Raha and A. Rusetsky, Eur. Phys. J. C **35** (2004) 349 [hep-ph/0402261].
- [17] J. Gasser, V. E. Lyubovitskij and A. Rusetsky, Phys. Rept. **456** (2008) 167 [arXiv:0711.3522 [hep-ph]].
- [18] T. Ishiwatari, C. Berucci, M. Cargnelli, J. Marton, H. Shi, E. Widmann, J. Zmeskal and M. Bazzi *et al.*, Acta Phys. Polon. B **45** (2014) 3, 787.
- [19] SIDDHARTA-2 Collaboration, Proposal at Laboratori Nazionali di Frascati of INFN, “The upgrade of the SIDDHARTA apparatus for an enriched scientific case,” 2010.
- [20] C. Berucci *et al.*, Letter of Intent for J-PARC, “Measurement of the strong interaction induced shift and width of the 1s state of kaonic deuterium,” 2013.
- [21] D. Gotta *et al.*, Lect. Notes Phys. **745** (2008) 165.
- [22] T. Strauch, F. D. Amaro, D. Anagnostopoulos, P. Buhler, D. S. Covita, H. Gorke, D. Gotta and A. Gruber *et al.*, Eur. Phys. J. A **47**, 88 (2011) [arXiv:1011.2415 [nucl-ex]].
- [23] V. Baru, C. Hanhart, M. Hoferichter, B. Kubis, A. Nogga and D. R. Phillips, Nucl. Phys. A **872** (2011) 69; Phys. Lett. B **694** (2011) 473
- [24] J. H. Hetherington and L. H. Schick, Phys. Rev. **137** (1965) B935; L. H. Schick and B. F. Gibson, Z. Phys. A **288** (1978) 307;
- [25] M. Torres, R. H. Dalitz and A. Deloff, Phys. Lett. B **174** (1986) 213; R. C. Barrett and A. Deloff, Phys. Rev. C **60** (1999) 025201. A. Deloff, Phys. Rev. C **61** (2000) 024004.
- [26] G. Toker, A. Gal and J. M. Eisenberg, Nucl. Phys. A **362** (1981) 405.
- [27] A. Bahaoui, C. Fayard, T. Mizutani and B. Saghai, Phys. Rev. C **68**, (2003) 064001 [arXiv:nucl-th/0307067]; T. Mizutani, C. Fayard, B. Saghai and K. Tsushima, Phys. Rev. C **87** (2013) 3, 035201 [arXiv:1211.5824 [hep-ph]].
- [28] N. V. Shevchenko, Phys. Rev. C **85** (2012) 034001 [arXiv:1103.4974 [nucl-th]].
- [29] N. V. Shevchenko, Nucl. Phys. A **890-891** (2012) 50 [arXiv:1201.3173 [nucl-th]].
- [30] N. V. Shevchenko and J. Revai, Phys. Rev. C **90** (2014) 034003 [arXiv:1402.3935 [nucl-th]].
- [31] R. Chand and R. H. Dalitz, Annals Phys. **20** (1962) 1.
- [32] S. S. Kamalov, E. Oset and A. Ramos, Nucl. Phys. A **690** (2001) 494 [nucl-th/0010054].
- [33] U.-G. Meißner, U. Raha and A. Rusetsky, Eur. Phys. J. C **47** (2006) 473 [nucl-th/0603029].
- [34] M. Doring and U.-G. Meißner, Phys. Lett. B **704** (2011) 663 [arXiv:1108.5912 [nucl-th]].
- [35] A. Gal, Int. J. Mod. Phys. A **22** (2007) 226 [nucl-th/0607067].
- [36] V. Baru, E. Epelbaum and A. Rusetsky, Eur. Phys. J. A **42** (2009) 111 [arXiv:0905.4249 [nucl-th]].
- [37] V. Baru, E. Epelbaum, C. Hanhart, M. Hoferichter, A. E. Kudryavtsev and D. R. Phillips, Eur. Phys. J. A **48** (2012) 69 [arXiv:1202.0208 [nucl-th]].
- [38] V. Baru, C. Hanhart, A. E. Kudryavtsev and U. G. Meißner, Phys. Lett. B **589** (2004) 118 [nucl-th/0402027].
- [39] M. Beneke and V. A. Smirnov, Nucl. Phys. B **522** (1998) 321 [hep-ph/9711391].
- [40] R. F. Mohr, R. J. Furnstahl, R. J. Perry, K. G. Wilson and H. -W. Hammer, Annals Phys. **321** (2006) 225 [nucl-th/0509076].
- [41] G. Fäldt, Phys. Scripta **16** (1977) 81
- [42] V. M. Kolybasov and V. G. Ksenzov, Zh. Eksp. Teor. Fiz. **71** (1976) 13; O. D. Dalkarov, V. M. Kolybasov and V. G. Ksenzov, Nucl. Phys. A **397** (1983) 498.
- [43] V. Baru and A. E. Kudryavtsev, Phys. Atom. Nucl. **60**, 1475 (1997) [Yad. Fiz. **60**, 1620 (1997)].
- [44] V. Lensky *et al.*, Eur. Phys. J. A **26** (2005) 107 [nucl-th/0505039].
- [45] H. Zankel, W. Plessas and J. Haidenbauer, Phys. Rev. C **28** (1983) 538.
- [46] A. D. Martin, Nucl. Phys. B **179** (1981) 33.
- [47] Z. H. Guo and J. A. Oller, Phys. Rev. C **87** (2013) 3, 035202 [arXiv:1210.3485 [hep-ph]].
- [48] M. Lacombe, B. Loiseau, J. M. Richard, R. Vinh Mau, J. Cote, P. Pires and R. De Tourreil, Phys. Rev. C **21** (1980) 861.